ELSEVIER

Computer-Aided Design 37 (2005) 1177–1189

COMPUTER-AIDED DESIGN

www.elsevier.com/locate/cad

# Theories and algorithms for 3-D root canal model construction

J. Dong[a,*], S.Y. Hong[b], G. Hasselgren[c]

[a]*Department of Mechanical Engineering Technology, Metro State College of Denver, 1201 5th Street, Denver, CO 80204, USA*
[b]*Department of Mechanical Engineering, National ChiaoTung University of Taiwan, Taiwan*
[c]*School of Dental and Oral Surgery, Columbia University, New York, NY, USA*

Received 4 April 2004

**Abstract**

This paper presents theories and algorithms for 3-D root canal model construction from 2-D X-ray images in a clinically practical way: (1) the geometrical rectification algorithm for correcting distorted 2-D X-ray images, (2) the transformation algorithms from 2-D X-ray image coordinate system to unified 3-D reference coordinate system, (3) the merging algorithms and theory for obtaining spatial root canal centerline by intersecting two surfaces with assumed parallel projection, and (4) the elliptical theory for exploring the root canal cross-sectional geometry. Using those theories and algorithms, three 3-D computer models constructed from teeth samples are presented to show the feasibility. The internal geometrical structure provided by 3-D computer graphics enables the clinician and the patient to comprehend root canal morphology efficiently, and the destructive access preparation before a clinician's inspection may be avoided during clinic practice.


*Keywords:* Root canal model; Radiographic image; Endodontic treatment

## 1. Introduction

The knowledge of 3-D morphology of root canals is important for dental clinician to perform successful endodontic treatment. Because the canal geometry may not be known without opening the canal, a destructive access preparation by removing parts of tooth crown and dentin is usually needed even before a clinician's inspection and diagnosis by 'feeling' with instruments. There is a need for a 3-D root canal model that will reveal the dimensions and geometry of the root canal, and display the locations of canal orifice and canal curvature in 3-D computer graphics. It will enable clinician to efficiently comprehend, diagnose, and record a problem within seconds or minutes, and to accurately shape and clean the root canal. With it, the destructive access preparation before a clinician's inspection can be avoided.

3-D Root canal model is also the foundation of computer-aided process planning for endodontic therapy. With known root canal shape and its geometrical characteristics, such as canal length, taper, curvature and orifice, a treatment planning system will be able to select the treatment tool (detail shape, size, and material), to determine the cutting parameters, and to generate tool paths for automated treatment.

In order to construct 3-D root canal model, this paper will explore the theories and algorithms needed for the modeling, then apply them in modeling some tooth samples.

## 2. Review of previous efforts and modeling strategy for clinical practice

Throughout this century, research on dental anatomy has to a great extent concentrated on exploration of the anatomy of root canal systems using different techniques [1–3]. Schneider [4] was one of the first to describe a reliable method of determining the curvatures from mesiodistal (from side to side of tooth) and buccolingual (front and back of tooth) views by means of radiographs. Methods to produce 3-D constructions of root canal morphology have been introduced in the last decade. Mayo et al. [5] introduced computer-assisted tomography in endodontic research to allow 3-D imaging of root canals. In this method the tooth was filled with a contrast medium, 'Ethiodol', and positioned on a grid (Everett Fixott). This method required six radiographs of each tooth. However, it is virtually impossible to take these X-rays in vivo with

* Corresponding author.
*E-mail address:* jdong@mscd.edu (J. Dong).

0010-4485//$ - see front matter © 2005 Elsevier Ltd. All rights reserved.
doi:10.1016/j.cad.2005.02.008

a 45–135° rotation of a root. Berutti [6] used a computerized reconstruction by taking serial sections photographs under stereomicroscope on extracted teeth. This method made it possible to analyze the changes in morphology of the root canal on an actual tooth during endodontic treatment. But these are destructive techniques, which cannot be used in clinics. Nielsen et al. [7] evaluated X-ray microtomography in endodontic research. Baume and Doll [8] published 3-D reconstruction of magnetic resonance imaging data using extracted teeth. These images were accurate to within ~0.1 mm. Dowker et al. [9] presented a 3-D root canal reconstruction using X-ray microtomography. The root canal systems of extracted teeth were reconstructed with a resolution of 40 μm cubic side length. These 3-D methods can be used in in vitro studies of root canal morphology. Dobó-Nagy et al. [10,11] described root canal axis with fourth order polynomial function by taken two images of extracted human teeth. Although this method needed only two images, these two images were taken by orthographic projection and situated perpendicularly, which is not possible when treating a patient. Although all of these methods improved our understanding of root canal anatomy, they cannot be used in clinical practice.

## 3. Reference fixture and image geometric rectification

### 3.1. Reference fixture design

Before a radiograph is taken a tooth reference fixture is clamped to the patients' teeth. This compact fixture is made of material with minimal radiation density, except for three imbedded reference points. These three reference points, serving as markers, are precision balls of known dimension and made of high-density material, so that X-rays won't penetrate through them. These three markers provide the reference coordinate frame in the radiographic image for accurate dimensional calibration, and 3-D modeling. The dental film (or sensor) is then placed between the tongue and the tooth. The three reference balls will be part of the image. A fixture design and placement in a human mouth is illustrated in Fig. 1.

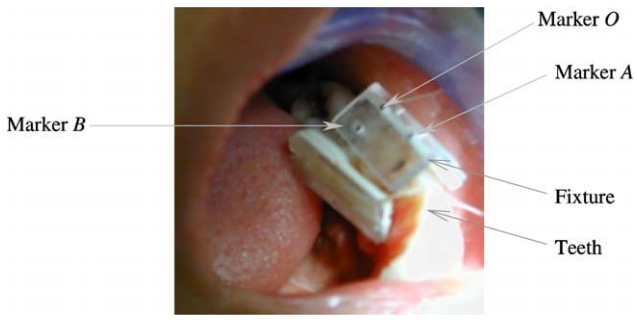


Fig. 1. The fixture design and placement in a human mouth.

### 3.2. Image geometric rectification

If an image is taken from an oblique direction, i e. the X-ray center beam is not perpendicular to the film it will cause image distortion. In order to minimize the geometric distortion of tooth image, two methods can be used. One is to use the film holder such as the one provided by the Digora system [12] to ensure a projection perpendicular to the film. Another is to find the virtual geometrical information in such an image that is perpendicular to X-ray central beam. The first method is simple and easy to achieve, the second method requires mathematical calibration and transformation with a marker as reference. Usually, the clinician places the film in one location and takes several images through changing the X-ray central beam direction and keeping the position of the film unmoved. If two images are needed, the dentist will take one image by using film holder, which ensures 90° angle between the X-ray center beam and film and then take another image mesially (towards middle) about 20° or distally (away from tooth) about 20°, or tilt the X-ray machine vertically, depending on which tooth is being examined. So the second image is usually an oblique image with distortion. Before modeling, geometrical rectification is needed to correct the distortion.

The three reference points of markers are precision balls of known dimension, they appear as white dots in the radiographic images. If the image is taken with orthogonal projection, i.e. the X-ray central beam is perpendicular to the film; these reference points will become three white circular dots. If the film is oblique with the X-ray central beam direction, these dots will instead appear as ellipses [13]. From the ratio of the long and short axis lengths of the ellipse, the oblique angle of the image film from X-ray imaging direction can be determined. Based on this a corrected image with true geometrical information can be found. This corrected image will be without distortion, and reflecting the true geometrical information, which is needed for 3-D modeling.

Fig. 2(a) illustrates the principle of the geometric rectification method. Because the distance between Markers *A* and *O* is longer than the distance between Markers *O* and *B*, there is less chance that Marker *A* overlaps with Marker *O* and *B*, Marker *A* is chosen to calculate the film oblique angle. Since the fixture is very close to the film with respect to the focal length of X-ray cone source, we consider this is the oblique parallel projection in the following calculation.

#### 3.2.1. Calculate major axis length of projective ellipse and its orientation angle

As shown in Fig. 2(b), the distance between any two pixel-points $(u^s, v^s)$ on an ellipse of oblique image is:

$$d = \sqrt{[(u_i^s)^2 - (u_j^s)^2]^2 + [(v_i^s)^2 - (v_j^s)^2]^2} \quad (1)$$

Through the iterative method, the maximum distance can be found which equals to major axis length of the ellipse,

$$2a = d_{\max}, \quad (2)$$

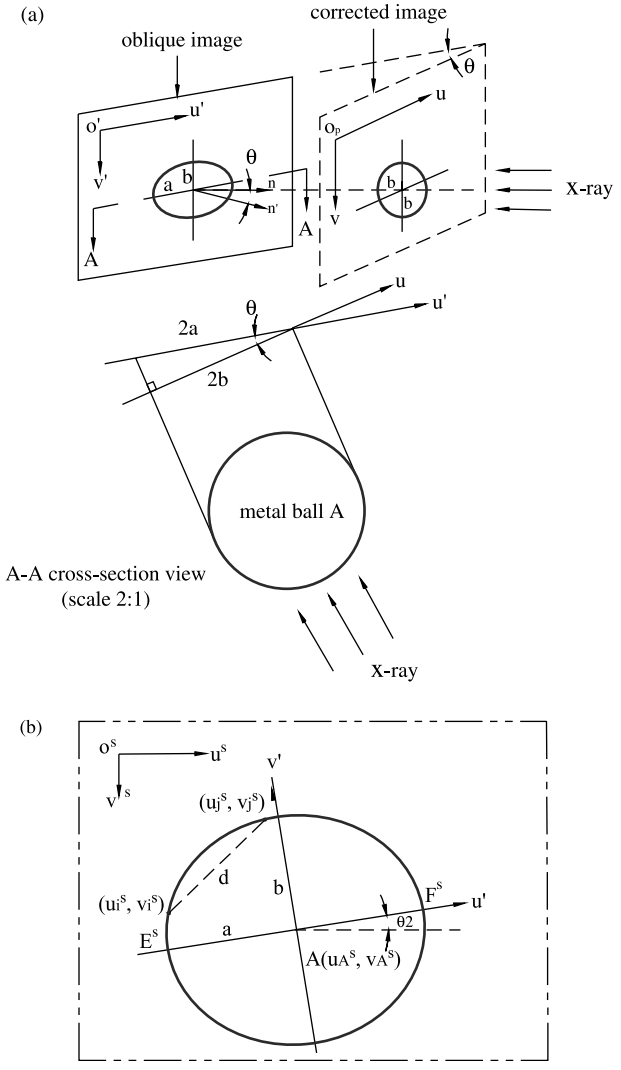


Fig. 2. (a) Image geometric rectification method using Marker *A* as reference. (b) Calculate major axis length of Market *A* projective ellipse in an oblique image.

and the coordinates of points *E* and *F* in the major axis of the ellipse can be found at the same time, so the orientation of major axis of the ellipse is

$$\tan\theta_2 = \frac{v_F^s - v_E^s}{u_F^s - u_F^s}; \tag{3}$$

where $\theta_2$ is the angle between ellipse major axis and *u* axis.

The center location of Marker *A* is obtained by the following equations

$$\begin{cases} u_A^s = \dfrac{1}{2}(u_E^s + u_F^s) \\ v_A^s = \dfrac{1}{2}(v_E^s + v_F^s) \end{cases} \tag{4}$$

*3.2.2. Find minor axis length of Marker A and oblique angle*

The half-length of minor axis of Marker *A* is the minimum distance between center point of Marker *A* and any point in ellipse, that is

$$b = \min(d_A), \tag{5}$$

where $d_A$ can be obtained from Eq (1) with $(u_j^s, v_j^s)$ substituted by Marker A center point coordinates $(u_A^s, v_A^s)$.

The oblique angle between the film plane normal direction and X-ray source direction is shown in Fig. 2(a)

$$\cos\theta = \frac{b}{a} \tag{6}$$

*3.2.3. Obtain geometrically corrected image and oblique transformation matrix S*

Once calculated the oblique angle $\theta$ the true dimension of the canal can be obtained in the corrected image, which is perpendicular to X-ray direction and obtained by rotating the film plane $\theta$ degree from oblique position to perpendicular position.

So the true dimensions in corrected image are expressed as below

$$\begin{bmatrix} u \\ v \\ 1 \end{bmatrix} = \begin{bmatrix} \cos\theta & 0 & 0 \\ 0 & 1 & 0 \\ 0 & 0 & 1 \end{bmatrix} \begin{bmatrix} u' \\ v' \\ 1 \end{bmatrix} = S \begin{bmatrix} u' \\ v' \\ 1 \end{bmatrix}, \tag{7}$$

where *S* is oblique transformation matrix,

$$S = \begin{bmatrix} \cos\theta & 0 & 0 \\ 0 & 1 & 0 \\ 0 & 0 & 1 \end{bmatrix} \tag{8}$$

Shown in Fig. 2(a) and (b), $u'$ and $v'$ are coordinates in major axis and minor axis of the ellipse, which is obtained by the following equations

$$\begin{bmatrix} u' \\ v' \\ 1 \end{bmatrix} = \begin{bmatrix} \cos\theta_2 & -\sin\theta_2 & 0 \\ \sin\theta_2 & \cos\theta_2 & 0 \\ 0 & 0 & 1 \end{bmatrix} \begin{bmatrix} u^s \\ v^s \\ 1 \end{bmatrix} = R_A \begin{bmatrix} u^s \\ v^s \\ 1 \end{bmatrix}, \tag{9}$$

where $R_A$ is major axis rotation matrix,

$$R_A = \begin{bmatrix} \cos\theta_2 & -\sin\theta_2 & 0 \\ \sin\theta_2 & \cos\theta_2 & 0 \\ 0 & 0 & 1 \end{bmatrix} \tag{10}$$

So the corrected image is calculated from original oblique image as

$$\begin{bmatrix} u \\ v \\ 1 \end{bmatrix} = SR_A \begin{bmatrix} u^s \\ v^s \\ 1 \end{bmatrix} = \begin{bmatrix} \cos\theta\cos\theta_2 & -\cos\theta\sin\theta_2 & 0 \\ \sin\theta_2 & \cos\theta_2 & 0 \\ 0 & 0 & 1 \end{bmatrix} \begin{bmatrix} u^s \\ v^s \\ 1 \end{bmatrix} \tag{11}$$

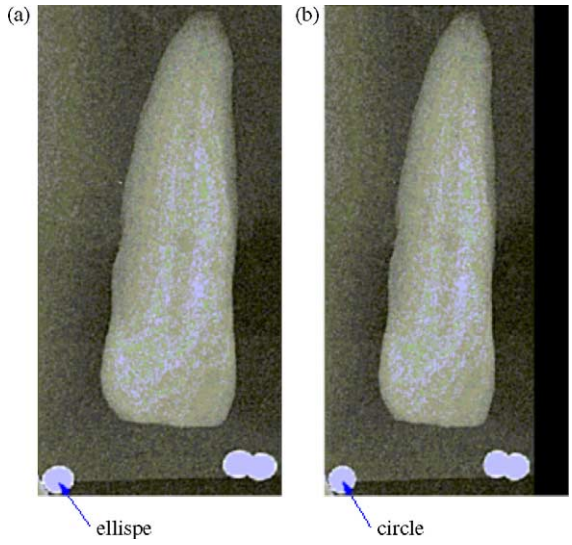


Fig. 3. Image geometrical rectification for maxillary left incisor. (a) Original image, (b) corrected image.

When the image is taken from mesial or distal direction, $\theta_2 = 0$, the corrected image is simplified as

$$\begin{bmatrix} u \\ v \\ 1 \end{bmatrix} = \begin{bmatrix} \cos\theta & 0 & 0 \\ 0 & 1 & 0 \\ 0 & 0 & 1 \end{bmatrix} \begin{bmatrix} u^s \\ v^s \\ 1 \end{bmatrix} = \begin{bmatrix} u^s \cos\theta \\ v^s \\ 1 \end{bmatrix}, \tag{12}$$

which is achieved by shrinking the original image in $u^s$ direction.

If the image is taken from upward or downward direction, $\theta_2 = -90°$, the corrected image is obtained by

$$\begin{bmatrix} u \\ v \\ 1 \end{bmatrix} = \begin{bmatrix} 0 & \cos\theta & 0 \\ -1 & 0 & 0 \\ 0 & 0 & 1 \end{bmatrix} \begin{bmatrix} u^s \\ v^s \\ 1 \end{bmatrix} = \begin{bmatrix} v^s \cos\theta \\ -u^s \\ 1 \end{bmatrix}, \tag{13}$$

which is the shrunk image in $v^s$ direction from the original image.

Fig. 3 gives an example image after geometrical rectification. (a) is the original (oblique) maxillary left incisor image taken from mesial 20°. (b) is the corrected image after geometrical rectification. From (b) one can see how Marker *A*'s projection becomes a circle compared to the ellipse in original image (a).

## 4. Transformation and calibration algorithms

Before constructing a 3-D root canal model, its 3-D coordinates should be found from a set of 2-D images, based on stereo principles and corresponding mathematical algorithms. There are four coordinate systems involved in the application of 3-D root canal modeling from 2-D images.

(1) Pixel coordinate system: $uvo_p$
Pixel coordinate system is an original 2-D image coordinate system where the image plane is perpendicular to the optical axis of X-ray central beam, or corrected image coordinate system after distortion rectification from oblique projection image. Its origin is located at left top corner of the image. The unit of this system is pixel. $P(u,v)$ represents a point in pixel coordinate system.

(2) Dimensional image coordinate system: xyo
Dimensional image coordinate system is a 2-D coordinate system. Its origin is the center point of Marker *O*. The unit of this coordinate system is millimeter. $P(x, y)$ represents a point in dimensional image coordinate system.

(3) X-ray perspective imaging coordinate system: $X_C Y_C Z_C O_C$
X-ray perspective imaging coordinate system refers to X-ray sources perspective projection system, which has the origin at X-ray source center and the optical axis (established by the center of the X-ray source) as $Z_C$ axis. The $X_C Y_C O_C$ plane is parallel to the image film. (According to dental terminology, the X-ray center beam refers to the optical axis). Any point in such coordinate system is expressed as $P(X_C, Y_C, Z_C)$.

(4) World coordinate system: $X_W Y_W Z_W O_W$
The fixture frame with three markers *A*, *B*, and *O* on a right angle bracket is defined as world coordinate system. *O* is the origin; *OA* denotes to $X_W$ axis, *OB* as $Y_W$ axis, $Z_W$ is perpendicular to the plane formed by *OA* and *OB*. Any point in world coordinate system is expressed as $P(X_W, Y_W, Z_W)$.

### 4.1. Transformation between world coordinate system and X-ray imaging coordinate system ($X_W Y_W Z_W O_W$–$X_C Y_C Z_C O_C$)

In 3-D space, an object has six degree of freedom. The motion of a rigid body can be divided into a transmission and a rotation. So the relationship between two 3-D coordinate systems can be described by a rotation matrix *R* and a transmission matrix *T* [14]. Suppose we wish to transform a point *H* with world coordinate $(X_W, Y_W, Z_W)$ into X-ray coordinate system, as shown in Fig. 4, the transformation form can be expressed as,

$$\begin{bmatrix} X_C \\ Y_C \\ Z_C \\ 1 \end{bmatrix} = R \begin{bmatrix} X_W \\ Y_W \\ Z_W \\ 1 \end{bmatrix} + T, \tag{14}$$

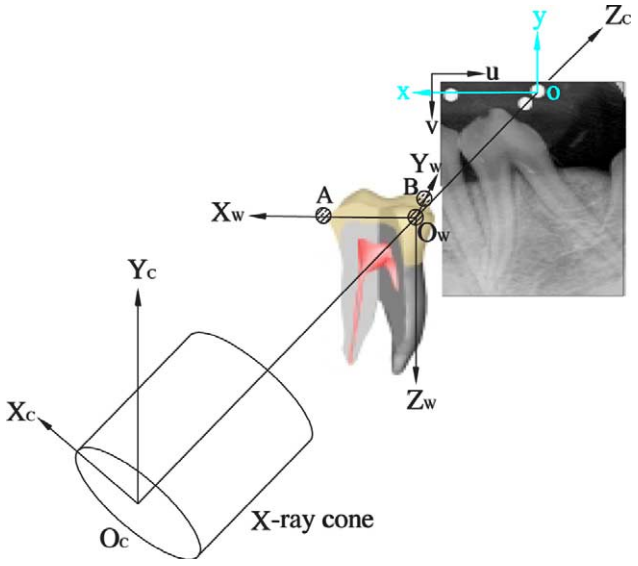


Fig. 4. Transformation among four coordinate systems during modeling.

where $[X_C, Y_C, Z_C]^T$ is the coordinate of same point $H$ in X-ray coordinate system. $T$ is transmission matrix from the origin in world coordinate system to the origin in X-ray coordinate system,

$$T = \begin{bmatrix} 1 & 0 & 0 & T_X \\ 0 & 1 & 0 & T_Y \\ 0 & 0 & 1 & T_Z \\ 0 & 0 & 0 & 1 \end{bmatrix} \tag{15}$$

$R$ is the rotation matrix by rotating point $H$ in an arbitrary direction. The calculation of $R$ can be simplified by rotating point $H$ about three coordinate axes and obtaining composite result. That is

$$R = R_\alpha R_\beta R_\gamma, \tag{16}$$

where $R_\gamma$ is the rotation matrix of rotating a point about $Z_C$-axis by an angle $\gamma$, which is measured clockwise when looking at the origin from a point on $+Z_C$ axis, $R_\alpha$ is the rotation matrix about $X_C$-axis by an angle $\alpha$, $R_\beta$ is the rotation matrix about the $Y_C$-axis by an angle $\beta$. $R_\gamma$, $R_\alpha$ and $R_\beta$ can be obtained in reference [15], so composite rotation matrix $R$ is the following

$$R = \begin{bmatrix} \cos\beta\cos\gamma & \cos\beta\sin\gamma & \sin\beta & 0 \\ \sin\alpha\sin\beta\cos\gamma - \cos\alpha\sin\gamma & \sin\alpha\sin\beta\sin\gamma + \cos\alpha\cos\gamma & \sin\alpha\cos\beta & 0 \\ \cos\alpha\sin\beta\cos\lambda + \sin\alpha\sin\gamma & \cos\alpha\sin\beta\sin\gamma - \sin\alpha\cos\gamma & \cos\alpha\cos\beta & 0 \\ 0 & 0 & 0 & 1 \end{bmatrix} \tag{17}$$

The matrices $T$ and $R$ describe the position and orientation of the X-ray central beam with respect to the fixture frame (world coordinate system). There are totally six independent variables in above transformation, three for rotation $R$, i.e. $\alpha$, $\beta$ and $\gamma$, and three for translation $T$, i.e. $T_X$, $T_Y$, $T_Z$, which are also called the extrinsic parameters of the X-ray cone in terms of computer vision [15].

If we want to use the unified matrix representation, Eq. (14) can be expressed in the following format:

$$H_C = RH_W + T \tag{18}$$

or

$$H_W = R^{-1}(H_C - T), \tag{19}$$

where $H_C$ is a column vector whose components are the transformed coordinates

$$H_C = \begin{bmatrix} X_C \\ Y_C \\ Z_C \\ 1 \end{bmatrix} \tag{20}$$

and $H_W$ is the column vector containing the original coordinates in the world coordinate system,

$$H_W = \begin{bmatrix} X_W \\ Y_W \\ Z_W \\ 1 \end{bmatrix} \tag{21}$$

### 4.2. X-ray perspective projection transformation ($X_CY_CZ_CO_C$–$xyo$)

The radiography is considered a system that performs a linear projective transformation from the projective space $P^3$ into the projective plane $P^2$ [16]. A perspective transformation, also called an imaging transformation, projects 3-D points or object onto an image plane. Any point in a 3-D X-ray coordinate system ($X_C$, $Y_C$, $Z_C$) is projected by perspective transformation onto an image plane with coordinate as ($x$, $y$). The relationship of ($x$, $y$) and ($X_C$, $Y_C$, $Z_C$) can be easily accomplished by the use of similar triangle.

$$x = \lambda\frac{X_C}{Z_C} \text{ and } y = \lambda\frac{Y_C}{Z_C}, \tag{22}$$

where $\lambda$ is the distance between X-ray source and the film, called focal length of X-ray central beam. It can be obtained either by fixture design or X-ray cone calibration.

The above equations can be rewritten linearly using homogeneous coordinates:

$$\begin{bmatrix} x \\ y \\ z \\ 1 \end{bmatrix} = \begin{bmatrix} 1 & 0 & 0 & 0 \\ 0 & 1 & 0 & 0 \\ 0 & 0 & 1 & 0 \\ 0 & 0 & \frac{1}{\lambda} & 0 \end{bmatrix} \begin{bmatrix} X_{\mathrm{C}} \\ Y_{\mathrm{C}} \\ Z_{\mathrm{C}} \\ 1 \end{bmatrix} \tag{23}$$

The above formula expresses the fact that the relationship between image and 3-D X-ray coordinates is linear in projective coordinates and can be written in matrix form as

$$h = PH_{\mathrm{C}}, \tag{24}$$

where

$$h = \begin{bmatrix} x & y & z & 1 \end{bmatrix}^T, \tag{25}$$

and $P$ is the perspective transformation matrix,

$$P = \begin{bmatrix} 1 & 0 & 0 & 0 \\ 0 & 1 & 0 & 0 \\ 0 & 0 & 1 & 0 \\ 0 & 0 & \frac{1}{\lambda} & 0 \end{bmatrix} \tag{26}$$

### 4.3. Image dimensional calibration (xyo–uvo$_p$)

Both the dimensional image coordinate system ($xyo$) and pixel coordinate system ($uvo_p$) are 2-D coordinate systems. The former has millimeter as unit and the latter has pixel value as unit. The coordinates of point ($u$, $v$) in pixel coordinate system can be found through the coordinates of same point ($x$, $y$) in the dimensional image system by the following equations

$$\begin{cases} u = u_o - \dfrac{x}{d_x} \\ v = v_o - \dfrac{y}{d_y} \end{cases}, \tag{27}$$

where ($u_o$, $v_o$) is the coordinate of the origin of metric image coordinate system in pixel coordinate system, which is the center location of Marker $O$. The quantities $d_x$ and $d_y$ can be interpreted as the size in millimeters of per horizontal and vertical pixel, respectively. They can be obtained by metal ball marker calibration.

From Eqs. (5) and (1), the half-length of minor axis $b$, which is the projective diameter of Marker $A$ in pixel, is known, and the real diameter of marker ball $d_{\mathrm{b}}$ is also known from fixture design, then $d_x$ and $d_y$ are

$$d_x = d_y = \text{scale} = \frac{d_{\mathrm{b}}}{2b} \text{ (mm/pixel)} \tag{28}$$

The Eq. (27) can be rewritten linearly using homogeneous coordinates,

$$h_P = Mh, \tag{29}$$

where

$$h_P = \begin{bmatrix} u & v & 1 & 1 \end{bmatrix}^T, \tag{30}$$

and $M$ is the transformation matrix from dimensional image to pixel coordinate system,

$$M = \begin{bmatrix} \dfrac{-1}{d_x} & 0 & u_O & 0 \\ 0 & \dfrac{-1}{d_y} & v_O & 0 \\ 0 & 0 & 1 & 0 \\ 0 & 0 & 0 & 1 \end{bmatrix} \tag{31}$$

The parameters $u_o$, $v_o$ along with focal length $\lambda$ do not depend on the position and orientation of the X-ray central beam in 3-D space, and they can thus be called intrinsic. Knowledge of the intrinsic parameters allows us to perform metric measurements in X-ray central beam systems, i.e. to compute the real length of root canal and real width of cross-section shape of canal in millimeter.

### 4.4. X-ray central beam calibration to obtain transformation matrices

The accuracy in interpreting the true dimension of root canal can be achieved by X-ray central beam self-calibration procedure. In the previous sections, explicit equations are obtained for the image coordinates ($u$, $v$) of a world point $H$ ($X_{\mathrm{W}}$, $Y_{\mathrm{W}}$, $Z_{\mathrm{W}}$). The implementation of these equations requires knowledge of the X-ray cone intrinsic and extrinsic parameters, and measurement of dimensions. The X-ray beam calibration is to determine intrinsic and extrinsic parameters so that images relative positions and orientations are known. The intrinsic parameter can be obtained by fixture design. The extrinsic parameters can be determined using a set of image points whose world coordinates are known. These points are markers and the computational procedure to obtain the X-ray beam extrinsic parameters using markers is the procedure to determine the transformation matrices.

Combining Eqs. (18), (24), and (29), any pixel point is expressed by

$$h_P = M\,P\,(RH_{\mathrm{W}} + T), \tag{32}$$

in which $M$ has two parameters of $u_o$ and $v_o$, $P$ has one parameter $\lambda$, $R$ has three parameters of $\gamma$, $\alpha$, and $\beta$, and $T$ has three parameters of $T_X$, $T_Y$ and $T_Z$, so there are totally nine unknown parameters. From Eq. (18) we know that each point gives two equations. So five markers are needed for the cone calibration. However, parameter $\lambda$ can be determined by fixture design or measured while taking the image, and $u_o$ and $v_o$ can be simply obtained by fixture design in this case, so only three markers (six unknown, two equations) are needed for the application. These three markers are Marker $A$, $O$ and $B$ in the fixture.

The coordinates of Marker $A$, $O$ and $B$ in world coordinate system are known from the fixture design, which are $(X_A, Y_A, Z_A)$, $(X_O, Y_O, Z_O)$, and $(X_B, Y_B, Z_B)$. Their 2-D pixel coordinates can be obtained from image edge map, they are $(u_A, v_A)$, $(u_O, v_O)$, and $(u_B, v_B)$. Substitute $A$, $O$ and $B$ coordinates into Eq. (32), we have the following formulations,

$$\begin{cases} \begin{bmatrix} u_A \\ v_A \\ 1 \\ 1 \end{bmatrix} = MP \left( R \begin{bmatrix} X_A \\ Y_A \\ Z_A \\ 1 \end{bmatrix} + T \right) \\ \begin{bmatrix} u_O \\ v_O \\ 1 \\ 1 \end{bmatrix} = MP \left( R \begin{bmatrix} X_O \\ Y_O \\ Z_O \\ 1 \end{bmatrix} + T \right) \\ \begin{bmatrix} u_B \\ v_B \\ 1 \\ 1 \end{bmatrix} = MP \left( R \begin{bmatrix} X_B \\ Y_B \\ Z_B \\ 1 \end{bmatrix} + T \right) \end{cases} \tag{33}$$

Resolve above six equations group, the ration angle $\alpha$, $\beta$, and $\gamma$, and displacement $T_x$, $T_y$ and $T_z$ can be found. The transformation matrices $R$ and $T$ therefore are obtained.

After X-ray cone calibration, the transform matrix, $M$, $P$, $R$ and $T$ are known, with reference to Eq. (19), the world coordinates of any image point can be mathematically expressed by

$$H_W = R^{-1}(P^{-1}\, M^{-1}\, h_P - T). \tag{34}$$

## 5. 3-D Root canal model construction

We consider 3-D root canal model construction to be finding the spatial root canal centerline and its cross-sectional geometry at each centerline point. By combining the centerline curve with each cross-sectional shape mathematically, a 3-D root canal model and its representation of the geometrical entity can be formulated.

### *5.1. -D curve of root canal centerline/root canal axis*

After image processing and analysis, the pixels representing the canal boundary can be obtained and saved in the database. Through the transformation from the image pixel coordinate system to world coordinate system, the canal centerline points or root axis points can be found in world coordinate system. The 2-D root canal centerline can be fitted into polynomials [17]. The spatial root canal centerline can be obtained by merging and intersecting two surfaces, which are represented by two 2-D canal centerline curves of image 1 and 2.

For a 3-D root canal centerline curve, suppose $l_1$ is its projection in image 1 and $l_2$ is its projection in image 2. These two planar algebraic centerline and their mathematical representations of polynomial are obtained in last section by planar root canal centerline curve fitting. Exerting a pull on $l_1$ toward to its X-ray source direction, a extrusion surface $surf_1$ is obtained. In the same way by stretch curve $l_2$ toward the corresponding X-ray direction, another extrusion surface $surf_2$ are obtained. Then the 3-D root canal centerline is obtained by calculating the intersection points of above two cylindrical surfaces $surf_1$ and $surf_2$.

In general, the problem of finding intersections for two surfaces leads to an under-determined nonlinear system of equations, independent of the nature of the surface representations being used. To compute four parameters of an intersection point, we have only three coordinate equations at our disposal. So we have to discretize the surface representation to reduce the number of degrees of freedom to three. Since the extrusion surface is formed by moving the generatrix along the curve, which consists of a group of spatial straight lines, we choose a parameter discretization method to find the intersection for two extrusion surfaces such that finding the intersection points of two extrusion surfaces can be achieved by calculating the intersections between a extrusion surface and a set of straight lines, the generatrix of another extrusion surface. The procedure is first to find the point in the root canal projection line $l_2$, stretch this point along the extrusion generatrix direction, to obtain its parametric equation. Secondly, to find another surface which is formed by root canal centerline $l_1$ in image 1, compute the intersection point $p_1$ between the straight line and above extrusion surface. In this way, we can calculate a set of intersection points of the straight lines and extrusion surface by a numerical method. The spatial root canal centerline is therefore obtained by fitting these intersection points with polynomial approximations.

In image 1, the generatrix of $surf_1$ can be obtained by stretch point $p_i(x_i^1, y_i^1)$ in $l_1$ toward generatrix direction (X-ray 1 source direction), and its parametric representation is:

$$\begin{cases} X_C^1 = x_i^1 \\ Y_C^1 = y_i^1 \\ Z_C^1 = q_1 \end{cases}, \tag{35}$$

where the superscript 1 of each coordinate denotes the coordinate obtained in taking X-ray image 1, $q_1$ is parameter and $x_i^1$ and $y_i^1$ are obtained from transformation matrix between image coordinate system and pixel coordinate system while taking X-ray image 1, that is

$$\begin{bmatrix} x_i^1 \\ y_i^1 \\ 1 \\ 1 \end{bmatrix} = M_1^{-1} \begin{bmatrix} u_i \\ v_i \\ 1 \\ 1 \end{bmatrix}, \tag{36}$$

where $M_1$ is transformation matrix from image 1 dimensional coordinate system to pixel coordinate system, shown in Eq. (31).

The generatrix equation $g_1$ of $surf_1$ in world coordinate system is

$$\begin{bmatrix} X^1 \\ Y^1 \\ Z^1 \\ 1 \end{bmatrix} = R_1^{-1} \begin{bmatrix} X_C^1 \\ Y_C^1 \\ Z_C^1 \\ 1 \end{bmatrix} = R_1^{-1} \begin{bmatrix} x_i^1 \\ y_i^1 \\ q_1 \\ 1 \end{bmatrix}, \tag{37}$$

where $R_1$ is the transformation matrix between world coordinate system and X-ray imaging 1 coordinate system, which are obtained by Eq. (17).

In image 2, the planar centerline point of root canal is obtained as $(u_i^2, v_i^2)$ in image 2 pixel coordinate system, the superscript 2 is related to image 2, does not means square.

After the transformation between dimensional image coordinate system and pixel coordinate system using Eq. (31), the root canal centerline point in image 2 can be represented in dimensional image coordinate system as

$$\begin{cases} x^2 = t_2 \\ y^2 = f_2(t_2) \end{cases}, \tag{38}$$

$$\text{where} \quad f_2(t) = \sum_{j=0}^{n} b_j \, t_2 \tag{39}$$

In 3-D X-ray imaging 2 coordinate system, the above root canal centerline curve represents an extrusion surface, which is:

$$\begin{cases} X_C^2 = t_2 \\ Y_C^2 = f_2(t_2), \\ Z_C^2 = q_2 \end{cases} \tag{40}$$

where $t_2$ and $q_2$ are parameters in X-ray imaging 2 coordinate system. Transform it to world coordinate system, the extrusion surface $surf_2$ can be written as

$$\begin{bmatrix} X^2 \\ Y^2 \\ Z^2 \\ 1 \end{bmatrix} = R_2^{-1} \begin{bmatrix} X_C^2 \\ Y_C^2 \\ Z_C^2 \\ 1 \end{bmatrix} = R_2^{-1} \begin{bmatrix} t_2 \\ f_2(t_2) \\ q_2 \\ 1 \end{bmatrix}, \tag{41}$$

where $R_2$ is transformation matrix from Eq. (17).

Let

$$\begin{bmatrix} X^1 \\ Y^1 \\ Z^1 \\ 1 \end{bmatrix} = \begin{bmatrix} X^2 \\ Y^2 \\ Z^2 \\ 1 \end{bmatrix}$$

to find the intersection point between $surf_2$ and generatrix $g_1$, that is

$$R_1^{-1} \begin{bmatrix} x_i^1 \\ y_i^1 \\ q_1 \\ 1 \end{bmatrix} = R_2^{-1} \begin{bmatrix} t_2 \\ f_2(t_2) \\ q_2 \\ 1 \end{bmatrix}, \tag{42}$$

where $q_1$, $q_2$ and $t_2$ are three variables, and are computed by resolving above three equations. Therefore, any point $(X_i, Y_i, Z_i)$ in spatial root canal centerline curve is obtained,

$$\begin{bmatrix} X_i \\ Y_i \\ Z_i \\ 1 \end{bmatrix} = R_1^{-1} \begin{bmatrix} x_i^1 \\ y_i^1 \\ q_1 \\ 1 \end{bmatrix} \text{ or } \begin{bmatrix} X_i \\ Y_i \\ Z_i \\ 1 \end{bmatrix} = R_2^{-1} \begin{bmatrix} t_2 \\ f_2(t_2) \\ q_2 \\ 1 \end{bmatrix} \tag{43}$$

Using the same procedure as above, a set points of spatial root canal centerline $(X_i, Y_i, Z_i)$, $i = 1, 2, \ldots, m$, can be found, in which $m$ is the total point number in root canal centerline. Based on the fitting algorithm to fit the above points using 3–5 order polynomials, then the spatial root canal centerline curve is represented in the following format,

$$\begin{cases} X = f(t) \\ Y = g(t), \\ Z = t \end{cases} \tag{44}$$

where $t$ is parameter, $f(t)$ and $g(t)$ are 3–5 order polynomial fitting functions.

Fig. 5 shows the spatial root canal centerline of maxillary left incisor obtained by calculating intersection line of two extrusion surfaces, (a) and (b) are different views. Surface 1 and surface 2 describe two different X-ray imaging directions. Surface 1 is formed by taking image 1 and surface 2 is formed by taking image 2. Two surfaces angle a $\theta$ degree-the oblique angle while taking image 2 relative to taking image 1.

### 5.2. Building 3-D root canal entity as elliptical cone

Strictly speaking, the X-ray source is a point source, and a planar X-ray image is a result of perspective projection of the tooth to the image plane. 3-D Model construction is therefore better handled by epipolarity technique. Since the dental film is very close to the real tooth (about a centimeter), compared to X-ray source (20–40 cm), the distortion and dimensional error is minimal, usually less than 1% [18]. This error can be further reduced by

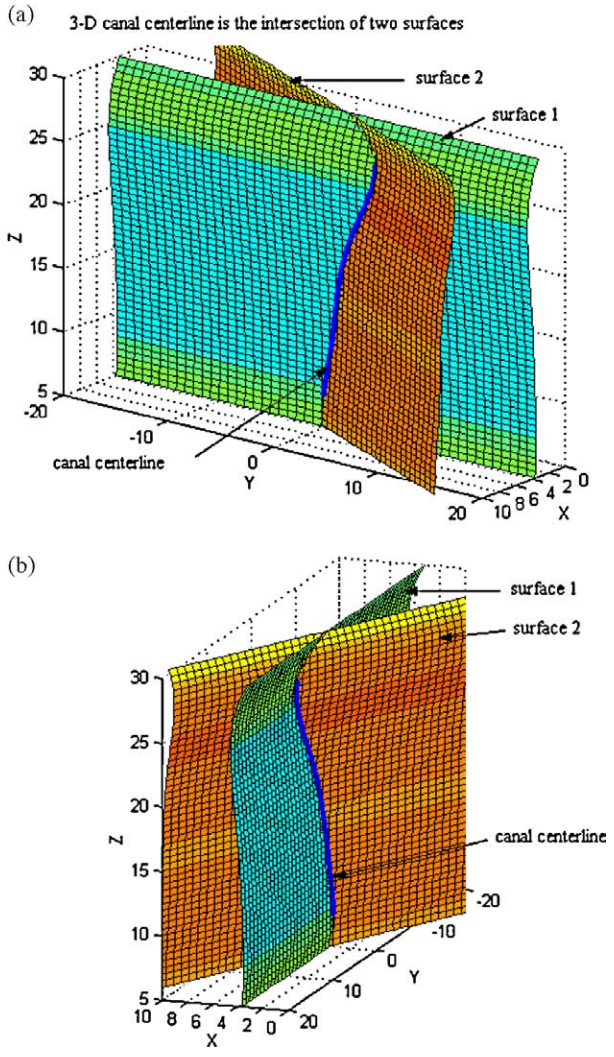


Fig. 5. Find the spatial root canal centerline of maxillary left incisor by intersecting two cylinder surface. (a) and (b) are different views.

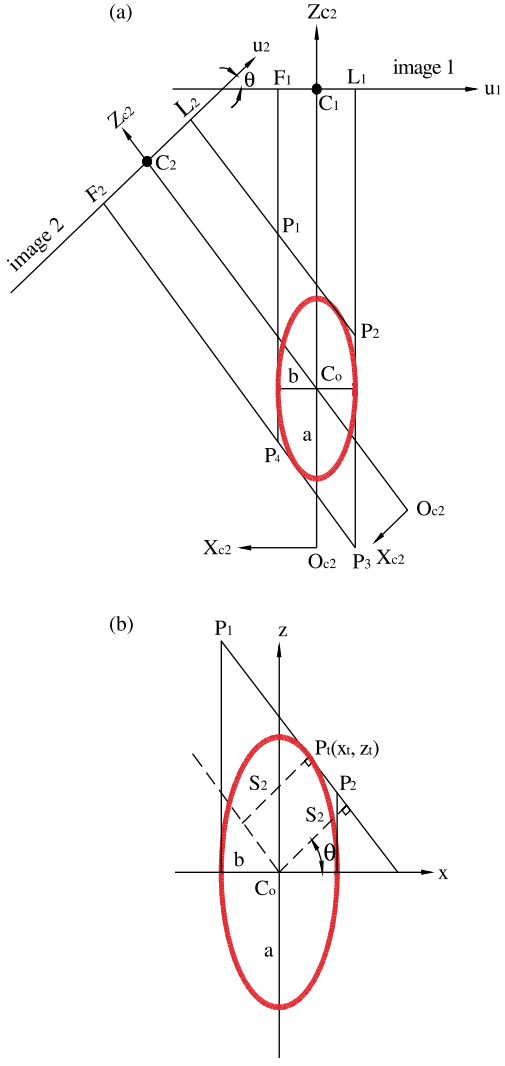


Fig. 6. (a) Formulation theory of 3-D root canal model with ellipse as cross-sectional shape, (b) calculation of half-length of major axis of an ellipse.

the dimensional calibration procedure using the three markers. To simplify calculations of the 3-D root canal model a parallel projection is assumed. The morphology study of the root canal shows that root canal cross-section trends to be circle and egg shaped. Therefore, in the following approach, the root canal cross-section shape is an ellipse, and the 3-D root canal entity is an ellipse cone.

Fig. 6 shows a cross-sectional root canal shape that is an ellipse. It is encapsulated in the rhombus and tangent to four edges of the rhombus. The rhombus is formed and controlled by two X-ray directions, X-ray 1 and 2, and four points in image 1 and 2, $F_1, L_1, F_2$, and $L_2$. $F_1$ is start point of root canal contour in image 1, $L_1$ is end point of root canal contour in image 1, $F_2$ is start point of root canal contour in image 2, and $L_2$ is end point of root canal contour in image 2. Two lines passed through $F_1$ and $L_1$ along the X-ray 1 imaging direction and two lines passed through $F_2$ and $L_2$ along the X-ray 2 imaging direction forms a rhombus, $P_1P_2P_3P_4$.

Usually Image 1 is taken from facial direction. From the knowledge of tooth anatomy, the root canal width is the shortest in facial image, so the minor axis is always lies on the $X_C$ axis, and its length $2b$ is equal to $F_1L_1$, that is,

$$b = \frac{1}{2}F_1L_1 = S_1 = \frac{1}{2}(x_{L1} - x_{F1}) = \frac{1}{2}\text{scale}(u_{L1} - u_{F1}) \tag{45}$$

The major axis lies on $Z_C$ axis, and its half-length $a$ is unknown and to be found. As shown in Fig. 6(b), line $P_1P_2$ is tangent to the ellipse at point $P_t(x_t, z_t)$. The ellipse and line $P_1P_2$ mathematical equations are

$$\begin{cases} \dfrac{x^2}{S_1^2} + \dfrac{z^2}{a^2} = 1 \\ x\cos\theta + z\sin\theta = S_2 \end{cases}, \tag{46}$$

where $S_2$ is the cross-sectional width of canal in Image 2, and calculated using Eq. (45) with $u_{L1}$, $u_{F1}$ substituted by $u_{L2}$, $u_{F2}$.

Solve above two equations to find expression of intersection points as below:

$$\begin{cases} x_{1,2} = \dfrac{S_2(a^2\sin^2\theta + b^2\cos^2\theta) - \sin\theta(a^2 S_2 \sin\theta \pm \Delta)}{\cos\theta(a^2\sin^2\theta + b^2\cos^2\theta)} \\ z_{1,2} = \dfrac{a^2 S_2 \sin\theta \pm \Delta}{a^2\sin^2\theta + b^2\cos^2\theta} \end{cases}, \tag{47}$$

where

$$\Delta^2 = a^2 S_1^2 \cos^2\theta(a^2\sin^2\theta + S_1^2\cos^2\theta - S_2^2) \tag{48}$$

Since the ellipse is tangent to line $P_1P_2$, there is only one intersection point between ellipse and line $P_1P_2$, that requires

$$\Delta = 0 \tag{49}$$

Resolve Eqs. (49) and (48), the half-length of major axis of ellipse $a$ is

$$a = \frac{\sqrt{S_2^2 - S_1^2\cos^2\theta}}{\sin\theta} \tag{50}$$

The $S_1$ is always less than $S_2$, so there is unique solution for $a$.

To represent the ellipse mathematically in world coordinate system, the ellipse parametric equation in cross-section $Y_C$ can be written as

$$\begin{cases} X_C = X_{CO} + b\cos t \\ Z_C = Z_{CO} + a\sin t \end{cases}, \tag{51}$$

where ($X_C$, $Y_C$, $Z_C$) is the X-ray 1 imaging coordinates of any point on the ellipse with specific canal height $Y_C$. ($X_{CO}$, $Y_C$, $Z_{CO}$) is the coordinates of ellipse center in the same canal height $Y_C$. The ellipse center in each height is the center of 3-D root canal model in the same cross-section. The centerline of 3-D canal model is the centerline of ellipse cone, and each center point in the centerline is the ellipse center in the same cross-section.

Through the transformation matrix $R_1$ between world coordinate system and X-ray 1 coordinate system, the ellipse mathematical equation in cross-section $Y = Y_{CO}$ can be obtained in the following format,

$$\begin{bmatrix} X \\ Y \\ Z \\ 1 \end{bmatrix} = R_1^{-1} \begin{bmatrix} X_C \\ Y_C \\ Z_C \\ 1 \end{bmatrix} = R_1^{-1} \begin{bmatrix} X_{CO} + b\cos t \\ Y_{CO} \\ Z_{CO} + a\sin t \\ 1 \end{bmatrix} \tag{52}$$

Change value $Y_{CO}$ from root canal foreman to canal orifice, to obtain a series of conic cross-section ellipses. These ellipses are combined into the spatial root canal model whose whole entity is an elliptical cone.

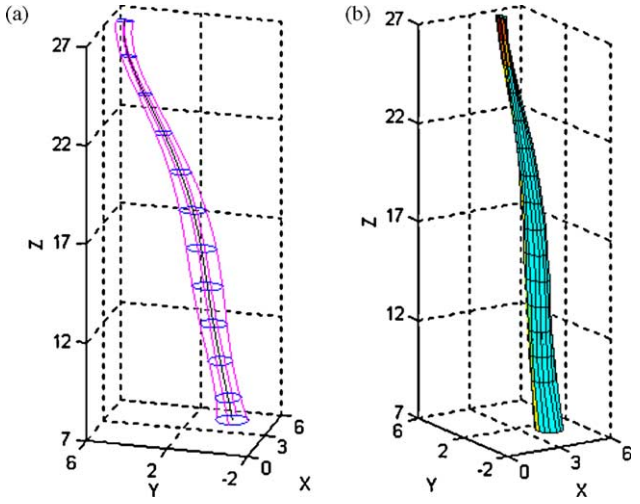


Fig. 7. 3-D Root canal model of maxillary left incisor. (a) 3-D Root canal ellipse cone with four contours (frame), (b) root canal solid model.

Fig. 7 shows an example of canal model for a maxillary left central incisor.

## 6. Examples of 3-D root canal model

Three typical sample teeth were chosen based on their different possible treatment procedures. The teeth were sterilized in formaldehyde, with calculus and soft tissue removed. All teeth had intact crowns and fully developed apices. For each specimen, two images were taken using the Digora photo stimulable phosphor sensors (Soredex, Finland) that are reusable image plates (normal size: 30×40 mm of image area and 466×628 pixels of image size). All image plates were placed perpendicularly to radiographic beam. Using a 20 cm X-ray tube all exposures were done at 70 kVp, 10 mA, and 16 impulses (Gendex X-ray machine). After exposure the sensors were processed in the Digora fmx system (Soredex, Finland). The Digora scanner moves the imaging plate with a conveyor and scans the surface of the plate with a laser beam at a frequency of about 30 scans per second. One readout pass consists of 628

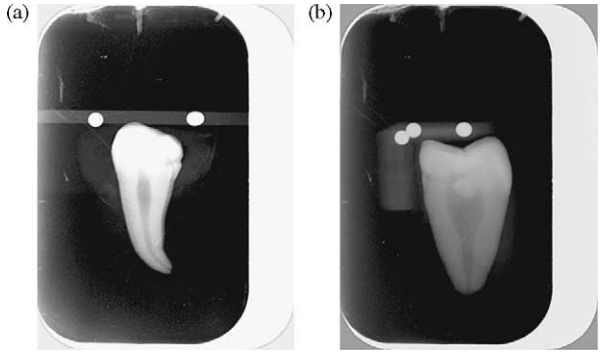


Fig. 8. Two images of human mandibular left premolar. (a) Facial view, (b) about 90° distal view.

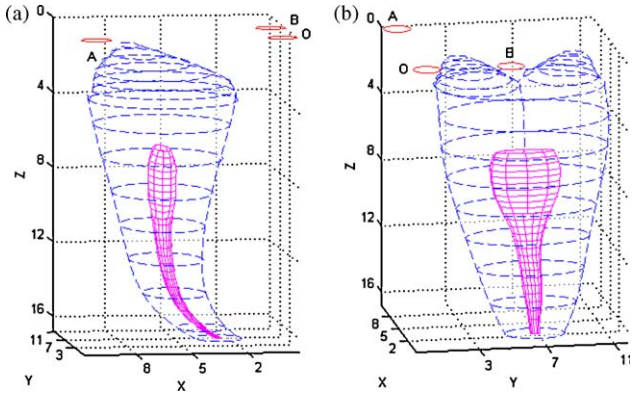


Fig. 9. Root canal model of human mandibular left premolar with chamber and tooth outlines.

scans. During each scan, the emitted light is measured 466 times. Each of these measurements represents one pixel of the final image. The measurements are displayed as an image on the computer screen and later stored in an image file of .bmp. The fixture was mounted on the tooth with Markers *A* and *O* close to the X-ray source and Marker *B* on the lingual side of the tooth.

Based on the theories and algorithms presented in the previous sections, three 3-D root canal models with chamber and teeth outlines were constructed.

### 6.1. Human mandibular left premolar with one root canal

This was a single-rooted, young permanent human posterior tooth-mandibular premolar with short tooth length and wide cross-sectional dimension. This tooth had one root canal with an elongated cross-sectional shape, like a 'ribbon', at each cross-sectional view of the canal. Two images were taken according to above descriptions. One was a facial view image with the central X-ray beam perpendicular to the plate. After the first image was taken, tooth is turned around 90° along the tooth's long axis. There another image is taken from a distal 90° angulation, also with the central X-ray beam perpendicular to the image plate. Two images are shown in Fig. 8. Using ellipses as

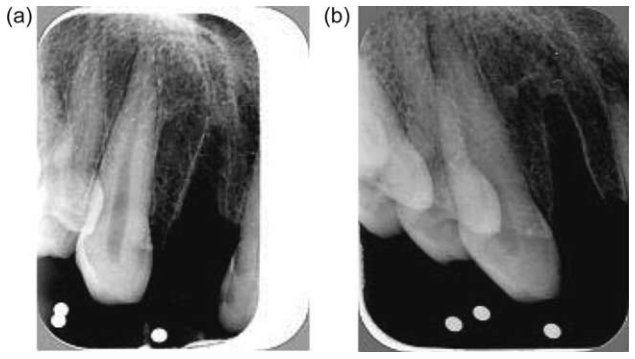


Fig. 10. Images of maxillary right canine. (a) Original facial view, (b) original mesial view.

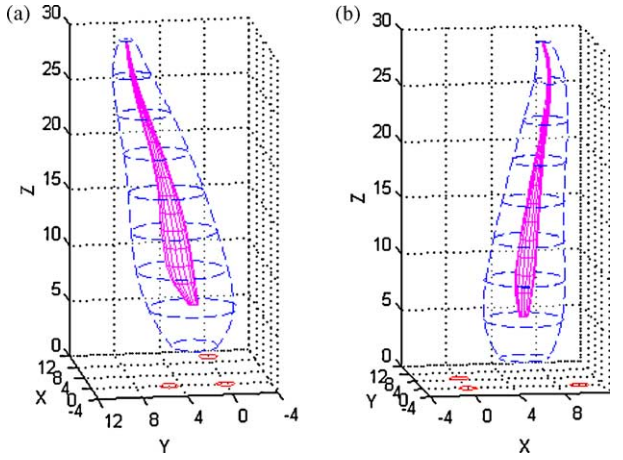


Fig. 11. Root canal model of maxillary right canine with tooth outlines.

canal cross-sectional shapes, the 3-D model of human mandibular premolar is constructed as shown in Fig. 9.

### 6.2. Human maxillary right canine with one root canal

This was a permanent human anterior tooth-maxillary canine in a skull. Two radiographic images were taken from the human skull of the maxillary right canine. One was a facial view, Fig. 10(a). Another one was a distal view of 20°, Fig. 10(b). In Fig. 10(b), three markers' projection became three ellipses, not circles, showing a distortion of the image. Therefore, a geometrical correction process was needed to correct the distortion. Using the geometric rectification algorithm stated in Section 3.2, the image orientation angle and oblique angle were calculated. The corrected distal view image was obtained by transforming the original image using the two angles. Based on facial image and corrected distal image, its 3-D canal model is constructed as shown in Fig. 11 with two different views.

### 6.3. Pig mandibular premolar with two root canals

The last sample tooth was a pig premolar It had two canals in two roots-one canal in each root. Modeling such canals helped us understand the spatial relationship of two canals in one tooth, i.e. their relative directions and orientations. A successful modeling of two canals in one tooth proved the possibility of modeling more than one canal at a time. The original pig premolar images were shown in Fig. 12, in which

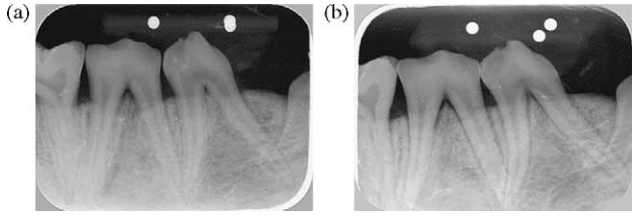


Fig. 12. Two original images of pig mandibular premolar. (a) Facial view, (b) distal view about 30°.

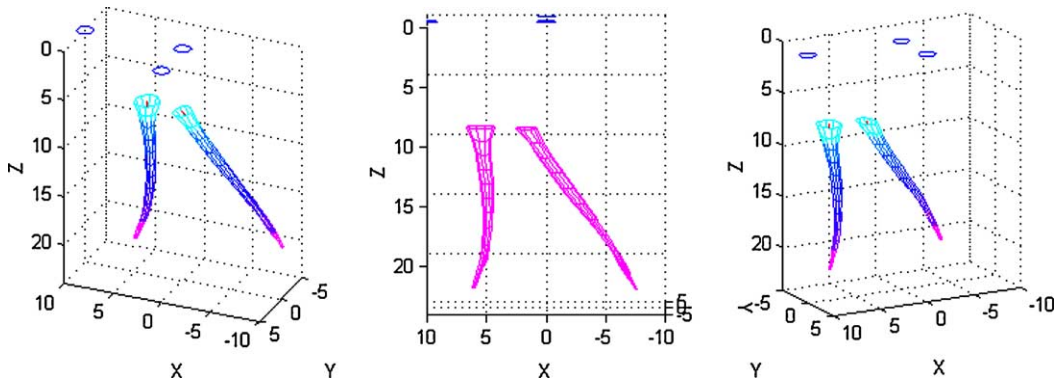


Fig. 13. Root canals model of pig mandibular premolar in three different views.

(a) is a facial view, and (b) is a distal view about 20°. The canal model was shown in Fig. 13 in two different views. Canal models with chamber and tooth outlines are shown in Fig. 14, also in two different views.

## 7. Conclusion

3-D Modeling of root canal is an important step to obtain information on the inner tooth anatomy prior to un-roofing of the pulp chamber. It is also the basis for computer aided endodontic treatment procedure planning [19]. The modeling algorithms and construction theories from two ordinary radiographic images were explored to obtain the 3-D root canal morphology in a way that is clinically possible. Three sample teeth were modeled to verify the feasibility of using the above theories and algorithms in clinic practice. The work in this paper is a pioneer effort to obtain 3-D root canal geometrical information from X-ray images available in clinical practice. The 3-D root canal model can be rotated and viewed from different angles. The clinician can see its internal structure by sectioning the 3-D model, which helps clinician treat root canal accurately and instantly. This is an important step towards achieving more precise root canal treatment.

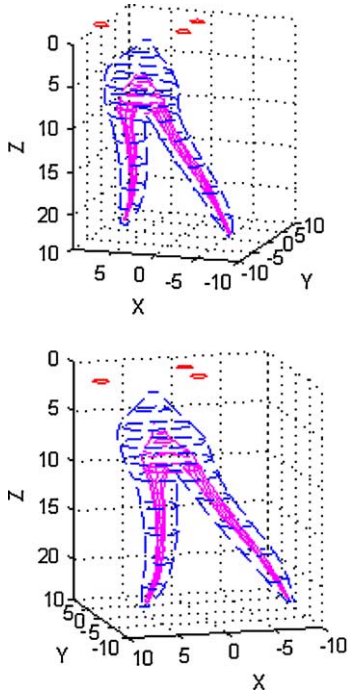


Fig. 14. Root canal model of pig mandibular premolar with chamber and tooth outlines in two different views.

## References

[1] Hess W. Anatomie der Wurzelkanale des menschlichen Gebisses mit Berücksichtigung der feineren Verzweigungen am Foramen apicale. Habilitationsschrift, Ulrich Co: Zürich; 1917.
[2] Fischer G. Uber die feinere Anatomie der Wurzelkanale menschlicher, Zahne. D. M. f. Z.; 1907.
[3] Meyer W. Die Anatomie der Wurzelkanale dargestellt an mikroskopischen Rekonstruktionsmodellen. Dtsch Zahnarztl Z 1970;25:1064–77.
[4] Schneider SW. A comparison of canal preparations in straight and curved canals. Oral Surg Oral Med Oral Pathol Oral Radiol Endod 1971;32:271–5.
[5] Mayo CV, Montgomery S, Rio C. A computerized method for evaluating canal morphology. J Endodon 1986;12:2–7.
[6] Berutti E. Computerized analysis of the instrumentation of the root canal system. J Endodon 1993;19:236–8.
[7] Nielsen RB, Alyassin AM, Peters DD, Carnes DL, Lancaster J. Microcomputered tomography: an advanced system for detailed endodontic research. J Endodon 1995;21:561–8.
[8] Bauman MA, Doll GM. Spatial reproduction of the root canal system by magnetic resonance microscropy. J Endodon 1997;23:49–51.
[9] Dowker SE, Davis GR, Elliot JC. X-ray microtomography: nondestructive three-dimensional imaging for in vitro endodontic studies. Oral Surg Oral Med Oral Pathol Oral Radiol Endon 1997;83:510–6.
[10] Dobó-Nagy C, Szabó J, Szabó J. A mathematically based classification of root canal curvatures on nature human teeth. J Endodon 1995;21:557–60.
[11] Dobó-Nagy C, Keszthelyi G, Szabó J, Sulyok P, Ledeczky G, Szabó J. Computeried method for mathematical descripton of three-dimensional root canal axis. J Endodon 2000;11:639–43.
[12] Digora fmx user's Manual and Installation Instruction, Soredex Orion Corporation, Helsinki, Finland, 1999.
[13] Gonzalez RC. Digital image processing. Reading, Massachusetts: Addison-Wesley publishing Company, Inc; 1987 p. 36–54, see also p. 176–183.
[14] Pavlidis T. Algorithms for graphics and image processing. Maryland: Computer Science Press, Inc; 1982 p. 66–72.

[15] Faugeras O. Three-dimensional computer vision: a geometric viewpoint. Cambridge, Massachusetts: The MIT Press; 1993 p. 37–76, see also p. 112–118, 165–242.
[16] Jain AK. Fundamentals of digital image processing. New Jersey: Prentice-Hall, Inc; 1989 p. 233–251 See also p. 347–375.
[17] Basri R. Generating views of 3D objects from viewer-centered representations, IFIP series on computer graphics, modeling in computer graphics: methods and applications, Springer-Verlag. p. 43–58.
[18] Rinn Corporation: intraoral radiography with rinn XCP/BAI instruments, form 1245–289, Rinn Corporation, Elgin, Illinois 60123–1819, 4–6.
[19] Dong J. Rule-based planning for automated endodontic treatment—from dental radiography, 3-D computer modeling to tool selection and path control. New York city, New York 10027: Dissertation of Columbia University; 2003 p. 138–184.

**Janet Dong** is an Assistant Professor of Mechanical Engineering Technology at Metro State College of Denver, USA. She received her PhD (2003) and MS (2001) degrees in Mechanical Engineering from Columbia University in the city of New York, and her MS (1990) and BS (1985) in Manufacturing Engineering from China. Dr Dong's research and educational interests include CAD/CAM, computer aided process planning and optimization, numerical control and automation, manufacturing technology, machine and instrument design, computer modeling, radiographic imaging processing, materials science, and dental endodontic treatment.

**Shane Y. Hong** is a Professor in the Department of Mechanical Engineering at National Chiao Tung University of Taiwan. Prior to returning Taiwan from USA., he was Professor of Mechanical Engineering at Columbia University from 1996–2004, and Associate Professor at Wright State University, 1990–1996; he was a Member of Technical Staff, Bell Laboratories, 1985–1990, and a Member of Research Staff, AT and T Princeton Engineering Research Center, 1983–1985. He received his BS degree (1975) from National Taiwan University, MS (1981) and PhD (1982) degrees from University of Wisconsin, USA, respectively.

**Gunnar Hasselgren** is a Professor and Director of the Division of Endodontics in the School of Dental and Oral Surgery at Columbia University in the city of New York, USA. He received his PhD degree (1977) in the University of Lund of Sweden, and his DDS from Columbia University (1989) and from School of Dentistry at Karolinska Institute (1963), respectively. He is a licensed practitioner in both Sweden and USA. His main areas of interest are hard tissue biology and studies related to clinical endodontics.